THERMO HYDRAULIC PERFORMANCE OF MICRO CHANNELS

NirmalyaBayal

Department of Mechanical Engineering, Haldia Institute of Technology, Haldia, INDIA.

Abstract: Recent development in micro energy and micro chemical systems has produced a need for greater understanding of fluid flow in small size channels. This paper investigates using a fourth order finite difference scheme for high subsonic and very low Reynolds number gas low through micro channels. The working fluids are nitrogen, hydrogen and helium. A two dimensional finite difference based micro scale flow model has been developed to predict efficiently the overall flow characteristics assuming isothermal first order slip flow. Reynolds numbers are very small of the order of 10^{-3} to 10^{-2} for the flows simulated; they can be safely assumed to be laminar. Based on this model, it has been concluded that the slip conditions results in a larger axial velocity than no slip conditions as the slip conditions implies less shear stress against boundaries.

Introduction:

Micron size mechanical devices are becoming more prevalent, both in commercial and in scientific industry. Applications of micro technology must utilize components or systems with micro scale fluid and heat transfer. There are several factors making the fluid flow and heat transfer behavior different in micro channels from that of normal sized channels. They can be largely summarized as:

(i) The compressibility and compressibility induced flow acceleration should be considered in evaluating the fluid flow characteristics in micro channels [1, 2].

(ii) The surface roughens, has a great influence on the flow and heat transfer characteristics for laminar flows as well as turbulent flows [1, 2].

(iii) The gas rarefaction. The degree of rarefaction is measured by the Knudsen number (Kn). The effect of rarefaction will lower the apparent viscosity and consequent friction factor as Kn is larger than 0.01 [2].

A large number of recent investigations have undertaken to study the fundamentals of micro channels. To analyze micro scale gas flows, various analytical and numerical studies have been performed [1-5]. Most numerical tools used in the literature include the Direct-Simulation-Monte Carlo (DSMC) or Navier-Stokes methods with slip boundary conditions. However, DSMC is still believed to be ineffective tool for low speed micro scale gas flows, due to its massive computational load and large unavoidable statistical fluctuations [3]. On the other hand, the Navier Stokes approach along with appropriate slip boundary conditions may analyze the velocity slip at wall surface and other characteristics in a most economical way without losing any accuracy of the flow modeling [3-5].

Since the mid 1980s, studies that came out of conventional methods started to emerge. The pioneer experimental investigation on gas flow in micro channel was done by Tuckerman and Pease [3]. This work has been considered as a major milestone in the development of micro scale heat sinks. Since that time, this technology has received con-

siderable attention in micro electronics and other major application areas, such as fuel cell systems and advanced heat sink designs. Slip flow, thermal creep, rarefaction, viscous dissipation, compressibility, intermolecular forces and other unconventional effects may have to be taken into account, preferably using only first principles such as conservation of mass, Newton's second law, conservation of energy, etc.

Governing Equations:

The standard two dimensional time dependent, compressible Navier-Stokes equations and energy equation has been used. The pressure is defined from equation of state. The governing equations are nonlinear in nature.

Conservation of mass:

$$\frac{\partial \rho}{\partial t}+\frac{\partial \rho u}{\partial x}+\frac{\partial \rho v}{\partial y}=0 \qquad (1)$$

Conservation of X-momentum:

$$\rho\left(\frac{\partial u}{\partial t}+u\frac{\partial u}{\partial x}+v\frac{\partial u}{\partial y}\right)=-\frac{\partial p}{\partial x}+\mu\left(\frac{4}{3}\frac{\partial^2 u}{\partial x^2}+\frac{\partial^2 u}{\partial y^2}+\frac{1}{3}\frac{\partial^2 v}{\partial x \partial y}\right) \qquad (2)$$

Conservation of Y-momentum:

$$\rho\left(\frac{\partial v}{\partial t}+u\frac{\partial v}{\partial x}+v\frac{\partial v}{\partial y}\right)=-\frac{\partial p}{\partial y}+\mu\left(\frac{4}{3}\frac{\partial^2 v}{\partial y^2}+\frac{\partial^2 v}{\partial x^2}+\frac{1}{3}\frac{\partial^2 u}{\partial x \partial y}\right) \qquad (3)$$

The pressure is defined using the perfect gas law:

$$p=\rho RT \qquad (4)$$

Boundary Conditions:

At the inlet a uniform velocity profile is assumed. Therefore $\partial u/\partial x=0$ and v=0. The pressure at the inlet is specified by pressure ratio. The temperature at the inlet is assumed to be same as the wall temperature.

At the outlet, the axial gradients of the flow variables are set to zero.

Slip Flow:

Slip flow occurs when gases are at low pressure or for flow in extremely narrow passages. The characteristics length scale of a micro channel is typically of the order of a few micrometers. We know that, mean free path of any gas generally varies from 10 to 100 *n*m, resulting in Knudsen number is in the slip flow regime ($0.001<Kn<0.1$) and is characterized as so called high Knudsen number flows. At high Knudsen number the Reynolds number is typically very small and has generally been recognized that the layer of gas immediately adjacent to the solid surface is no longer at rest relative to the solid surface but has a finite slip velocity. The continuum assumptions are not valid near the solid boundaries. Therefore slip flow which represents the rarefaction effects is modeled. In the presence of wall-normal and tangential temperature gradients, for an ideal gas the complete slip-flow (first order) will be in non-dimensional form [4]:

$$u^*_{gas}-u^*_{wall}=\frac{2-\sigma_v}{\sigma_v}Kn\left(\frac{\partial u^*}{\partial y^*}\right)_w \qquad (5)$$

For continuum flow, Kn'!0, above equation reduces to the familiar no-slip conditions.

The temperature jump boundary condition is:

$$T^*_{gas}-T^*_{wall}=\frac{2-\sigma_T}{\sigma_T}\left[\frac{2\gamma}{\gamma+1}\right]\frac{Kn}{Pr}\left(\frac{\partial T^*}{\partial y^*}\right)_w \qquad (6)$$

where, $\sigma_v=\frac{\tau_i-\tau_r}{\tau_i-\tau_w}$; Tangential momentum accommodation coefficient (TMAC).

$\sigma_T = \frac{dE_i - dE_r}{dE_i - dE_w}$; Thermal-accommodation coefficient.

Subscripts i,r,w stands for incident, reflected and solid wall conditions respectively; τ is a tangential momentum flux. dE is the energy flux.

For real walls, a portion of the momentum of the incident molecules is lost to the wall and a portion is retained by the reflected molecules. TMAC is defined as the fraction of molecules reflected diffusively.

Methodology:

The governing equations are nonlinear in nature. The numerical computation was carried out by solving the governing equations along with boundary conditions by forth order accurate finite difference implicit scheme with uniform grids. Convergence and accuracy were obtained by MacCormack multi step (intermediate step between n and n+1) scheme. Stability has been checked for every grid points for each iteration by following empirical formulas.

$$\Delta t \le \frac{\sigma(\Delta t)_{CFL}}{1+2/\mathrm{Re}_\Delta} \qquad \text{Where } \sigma \cong 0.7-0.9 \tag{7}$$

$$(\Delta t)_{CFL} \le \left[\frac{|u|}{\Delta x}+\frac{|v|}{\Delta y}+a\sqrt{\frac{1}{\Delta x^2}+\frac{1}{\Delta y^2}}\right]^{-1} \tag{8}$$

$$\mathrm{Re}_\Delta = \min\left(\mathrm{Re}_{\Delta x}, \mathrm{Re}_{\Delta y}\right) \ge 0, \quad Re_{\Delta x} = \frac{\rho|u|\Delta x}{\mu},$$

$$\mathrm{Re}_{\Delta y} = \frac{\rho|v|\Delta y}{\mu} \tag{9}$$

The flow is assumed to be two dimensional and does not varies in z-direction is assumed negligible. The governing equations for this study are the continuity equation, unsteady two-dimensional compressible Navier-Stokes equation and the equation of state. Two sets of boundary conditions on the channel wall, a slip wall and a no-slip wall are employed in the simulation to study their effects on the results. The solution procedure starts by applying the initial guess values and obtaining a converged solution by iteration. The iterations were continued until the sum of residuals for all computational cells became negligible i. e. max $\left|\left(u^{n+1}-u^n\right)/u^{n+1}\right| \le 10^{-5}$ is satisfied, where u is the velocity in the x direction and n denotes the number of the time steps. The distribution of cells in the computational domain was determined from a series of tests with a different number of cells in axial and transverse directions. A uniformly distributed 5000x30 grid is found to be adequate and has been used throughout the study. Accuracy of the scheme has been studied by varying the grid dimensions up to 6000 x 50.

Model Dimensions:

Several experimental and numerical results have been documented for this popular geometry [4]. Table 1 lists the dimensions of the micro channel.

Table I: Model dimensions:

Length L	3000 μm
Width W	40 μm
Height H	1.2 μm

Results and Discussions:

Gas flows are flows of compressible fluid that flow under conditions of expansion with changes in its density, pressure, velocity and temperature along the axial direction. In micro channel flows, the velocity of the molecules near the wall decreases and the molecules near the centerline accelerates to keep the mass flow rate constant. Figure 1

shows the axial velocity at three different axial locations with a pressure ratio Pr= 2.65. The axial velocity has been non-dimensionalized with the velocity of sound. To check the accuracy of the present work, the fully developed velocity profile has been compared with the numerical results of Chen *et al.* [4]. It is important to note that Chen *et al.* utilized an explicit finite difference method on a 6000 x 23 grids, while 5000 x 30 grids have been used for this present numerical simulations. An accommodation coefficient σ_v =0.85 has been incorporated.

It is visible from figure 1 that at downstream velocity increases with a corresponding increase in wall velocity due to slip effect. In order to satisfy the conservation of mass along the channel, in the direction of flow, the flow is accelerated to make up the change in density that result from the decrease of the pressure. In case of compressible flow the velocity is obviously accelerated because local bulk density decreases due to low local pressure there and the average velocity increases. This is due to the volume expansion of the gas caused by the pressure drop. Consequently fully developed flow never occurs due to this compressibility effect even if the micro channel is very long. The present model, it has been assumed that if the axial velocity gradient is less that 10^{-6}, the flow is fully developed. From this figure it is also clear; velocity slip increases in the downstream direction.

The dependence of velocity distributions on the increase of Knudsen number is plotted in figure 2. It has been observed from this figure that, as the Knudsen number increases, the maximum velocity at the centre of the duct decreases and the shape of velocity distributions are getting flatter, but the tangential slip velocity at the wall increases. The local maximum velocity is reduced while slip velocity gets higher with the increase of Knudsen number. Four separate Knudsen numbers (*Kn* =0.0. 0.05, 0.10 and 0.15) have been considered and Reynolds number for the numerical simulation has been taken as 100. To get the longest hydrodynamic length *Re*=100 has been chosen. From this figure it is also depicted that, for the fully developed flow, the traditional parabolic curve is still obtained. It is well known that for fully developed flow the axial velocity gradient $\frac{\partial u}{\partial x} = 0$, and that transverse component $v = 0$. It has been observed from figure 2, that at *Kn*=0.0, u/u_{av} =1.5. This implies no slip at the wall. As the Knudsen number increases u/u_{av} decreases. This is due to slip condition. As *Kn* increases slip length also increases. From this figure it is also seen that non-dimensionalised velocity remains invariant with respect to Knudsen number at two different locations A and B at y/H = ±0.4. Noting that with the present slip flows at the wall, the velocity is no longer zero near the wall. The slip condition results in larger axial velocity than the no slip condition as slip condition implies less shear stress against the wall. That is why fully developed flow has occurred much earlier. This shows that as *Kn* increases rarefaction effects become more pronounced.

The effect of slip and no-slip boundary conditions on centerline of the channel (at y=0) is shown in figure 3 for four different pressure ratios. The slip condition solutions consistently show a higher magnitude of velocity than no-slip condition. This is expected since the slip condition implies less shear stress against the wall. It is seen from this figure that at lower pressure ratio for (Pr=1.35) the centerline velocity distribution is almost linear. As the pressure ratio in-

creases, the centerline velocity distribution becomes nonlinear. It is seen that the nonlinear distribution of the velocity is dependent on the pressure distribution and hence varies for different pressure ratios. As the pressure ratio increases, the nonlinearity of the streaming velocity distribution becomes prominent. Clearly, an increase in pressure ratio shows increasing divergence in the pressure distribution between the slip and no-slip wall solutions. The effect is the most prominent for Pr=2.65 where the maximum percentage difference in the pressure distribution between two predictions is near about 12%.

Wall slip depends on Knudsen number and molecular mean free path (λ). Comparisons of slip length between nitrogen and helium have been made in figure 4. It is evident from this figure that slip length of helium is larger as compared to nitrogen. This is because of molecular mean free path. It is also observed; as Knudsen number increases, slip length also increases almost linearly, but the rate of increase is more for helium flow. Slip length also depends on wall roughness. As roughness increases, momentum accommodation coefficient also increases. Figure 5 represents slip length for different accommodation coefficient. It is evident from this figure that as σ_v increases, slip length decreases.

Conclusions:

Rarefaction and compressibility are related and have a pronounced effect on fluid flow characteristics. The effect of rarefaction and compressibility are a function of Reynolds number. For lower Reynolds numbers, the effect of Knudsen number is dominant and for higher Reynolds number, the effect of Mach number is more important. Due to small characteristic length, the departure from continuum becomes more pronounced and there exists a finite slip velocity at the wall. The mean free path becomes larger with a reduction in pressure and Knudsen number becomes higher. As Knudsen number increases, the departure from continuum becomes significant. As Knudsen number increases, rarefaction effects become more important and slip length increases. Due to molecular mean free path, slip length of helium is more as compared to nitrogen. As surface roughness increases, slip length decreases

References:

1. P. Y. We and W. A. Little, 1983, "Measurement of friction factors for the flow and gases in very fine channels used for micro miniature Joule Thomson refrigeration", *Cryogenics*, vol. 23, pp. 273 – 277.
2. J. N. Pfahler, J. Harley, H. Bau and J. Zemel, 1991, "Gas and liquid flow in small channels", *ASME DSC*, vol. 32, pp. 49 - 60.
3. G. Bird, 1994, *Molecular Gas Dynamics and Direct Simulation of Gas Flows*, Oxford Science, Avon, U. K.
4. A. Beskok, G. E. Karniadakis and W Trimmer, 1996, "Rarefaction and Compressibility Effects in Gas Micro Flows", *J. Fluids Eng.*, vol. 118, pp. 448-456.
5. E. S. Piekos and K. S. Breuer, 1996, "Numerical Modeling of Micromechanical Devices Using the Direct Simulation Monte Carlo Method", *J. Fluids Eng.*, vol. 118, pp. 464-469.

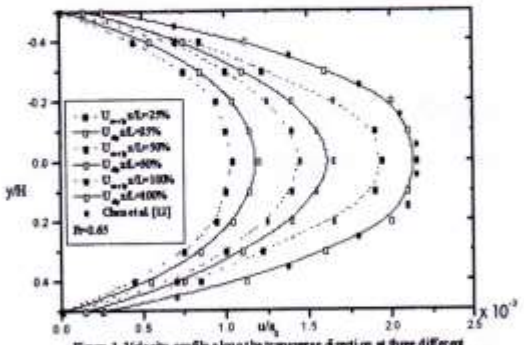

Figure 1. Velocity profile along the transverse direction at three different axial locations of nitrogen flow subjected to slip and no slip boundary conditions.

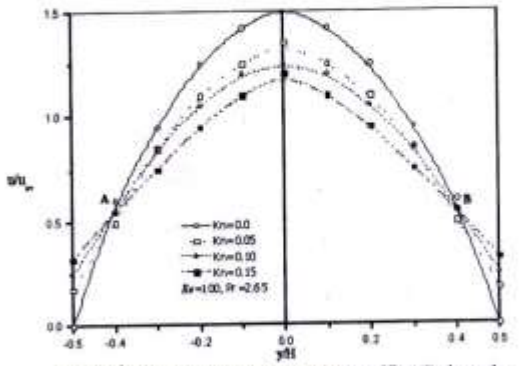

Figure 2. Fully developed velocity profile for nitrogen flow at different Knudsen numbers.

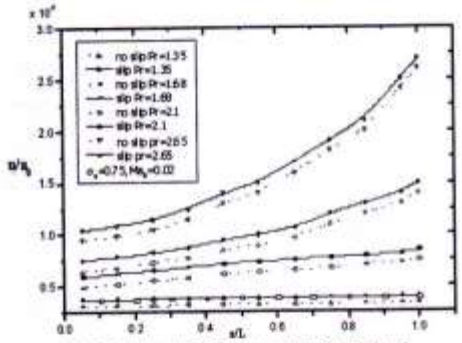

Figure 3. Centerline velocity distribution normalized with speed of sound. Solutions have been compared for slip and no slip conditions for four different pressure ratios.

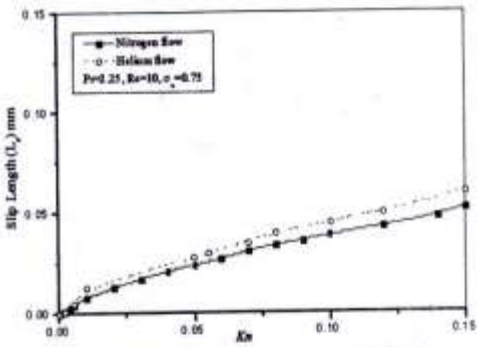

Figure 4. Comparison of slip length (L_s) between nitrogen and helium flow at different Knudsen numbers.

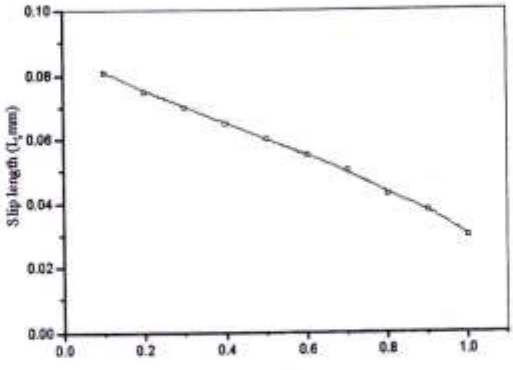

Figure 5. Slip length at different accommodation coefficients.